J|A|C|S
ARTICLES
Published on Web 12/13/2001

Structure of Docosahexaenoic Acid-Containing Phospholipid Bilayers as Studied by ^{2}H NMR and Molecular Dynamics Simulations

Thomas Huber,[‡] Kannan Rajamoorthi,[‡,§] Volker F. Kurze,[⊥,#] Klaus Beyer,[⊥] and Michael F. Brown*[,‡]

Contribution from the Department of Chemistry, University of Arizona, Tucson, Arizona 85721, and Lehrstuhl für Stoffwechselbiochemie der Universität München, D-80336 München, Germany

Received June 5, 2001

Abstract: Polyunsaturated phospholipids are known to be important with regard to the biological functions of essential fatty acids, for example, involving neural tissues such as the brain and retina. Here we have employed two complementary structural methods for the study of polyunsaturated bilayer lipids, viz. deuterium (^{2}H) NMR spectroscopy and molecular dynamics (MD) computer simulations. Our research constitutes one of the first applications of all-atom MD simulations to polyunsaturated lipids containing docosahexaenoic acid (DHA; 22:6 *cis*-$\Delta^{4,7,10,13,16,19}$). Structural features of the highly unsaturated, mixed-chain phospholipid, 1-palmitoyl-2-docosahexaenoyl-*sn*-glycero-3-phosphocholine (PDPC), have been studied in the liquid-crystalline (L_α) state and compared to the less unsaturated homolog, 1-palmitoyl-2-oleoyl-*sn*-glycero-3-phosphocholine (POPC). The ^{2}H NMR spectra of polyunsaturated bilayers are dramatically different from those of less unsaturated phospholipid bilayers. We show how use of MD simulations can aid in interpreting the complex ^{2}H NMR spectra of polyunsaturated bilayers, in conjunction with electron density profiles determined from small-angle X-ray diffraction studies. This work clearly demonstrates preferred helical and angle-iron conformations of the polyunsaturated chains in liquid-crystalline bilayers, which favor chain extension while maintaining bilayer flexibility. The presence of relatively long, extended fatty acyl chains may be important for solvating the hydrophobic surfaces of integral membrane proteins, such as rhodopsin. In addition, the polyallylic DHA chains have a tendency to adopt back-bended (hairpin-like) structures, which increase the interfacial area per lipid. Finally, the material properties have been analyzed in terms of the response of the bilayer to mechanical stress. Simulated bilayers of phospholipids containing docosahexaenoic acid were less sensitive to the applied surface tension than were saturated phospholipids, possibly implying a decrease in membrane elasticity (area elastic modulus, bending rigidity). The above features distinguish DHA-containing lipids from saturated or monounsaturated lipids and may be important for their biological modes of action.

Introduction

Polyunsaturated fatty acids (PUFAs)[1] are derived from essential fatty acids (EFAs) and are implicated in key biological functions such as retinal and neural development,[2] learning, neurological dysfunctions including Alzheimer's disease, Parkinson's disease, Zellweger's syndrome, and schizophrenia,[3] and diseases including atherosclerosis and cancer.[4] Most interestingly, a single PUFA constituent of membrane phospholipids, namely docosahexaenoic acid (22:6ω3, DHA), has been suggested to be implicated in many of these effects. Recently, apoptosis[5] as well as cystic fibrosis[6] have also been shown to be influenced by DHA. The latter is the most common end product of the biosynthetic pathway for polyunsaturation of the ω3 series of EFAs, starting from α-linolenic acid. Phospholipids containing DHA have been reported to constitute as much as 15−25 mol % of the lipids of the gray matter of the human brain.[7] In the mammalian visual system, a part of the brain particularly suited for the research at the molecular level, DHA comprises 47 mol % of the acyl chains of the retinal rod outer segment phospholipids,[7] with as much as 63 mol % present in some species.[8]

* To whom correspondence should be addressed. Department of Chemistry, University of Arizona, Tucson, AZ 85721. Phone: 520-621-2163. Fax: 520-621-8407. E-mail: mfbrown@u.arizona.edu.

‡ University of Arizona.

§ Present address: BASF Agro Research, P. O. Box 400, Princeton, NJ 08543-0400.

⊥ Lehrstuhl für Stoffwechselbiochemie der Universität München.

Present address: Klinikum der Universität München, Germany.

(1) Abbreviations: AA, arachidonic acid; DHA, docosahexaenoic acid; DPPC, 1,2-dipalmitoyl-*sn*-glycero-3-phosphocholine; egg PC, egg yolk phosphatidylcholine; MD, molecular dynamics; NMR, nuclear magnetic resonance; PC, phosphatidylcholine; PDPC, 1-palmitoyl-2-docosahexaenoyl-*sn*-glycero-3-phosphocholine; PDPC-d_{12}, 1-palmitoyl-2-vinylperdeuteriodocosahexaenoyl-*sn*-glycero-3-phosphocholine; PDPC-d_{31}, 1-perdeuteriopalmitoyl-2-docosahexaenoyl-*sn*-glycero-3-phosphocholine; POPC, 1-palmitoyl-2-oleoyl-*sn*-glycero-3-phosphocholine; POPC-d_9, 1-palmitoyl-2-oleoyl-*sn*-glycero-3-trideuteriomethyl-phosphocholine; POPC-d_{31}, 1-perdeuteriopalmitoyl-2-oleoyl-*sn*-glycero-3-phosphocholine; PUFA, polyunsaturated fatty acid; SDPC, 1-stearoyl-2-docosahexaenoyl-*sn*-glycero-3-phosphocholine; SOPC, 1-stearoyl-2-oleoyl-*sn*-glycero-3-phosphocholine.

(2) Neuringer, M. *Am. J. Clin. Nutr.* **2000**, *71*, 256S−267S.

10.1021/ja011383j CCC: $22.00

It is known that PUFAs such as DHA are typically constituents of membrane phospholipids, which are found as structural components of biomembranes. Consequently, knowledge of their structural properties is necessary to understand their roles in biological functions at the molecular level. In eukaryotic cells, PUFAs pertaining to the ω6 and ω3 series of homologous fatty acids are of particular relevance. Arachidonic acid (20:4ω6, AA) and DHA are for some animals the main polyunsaturated metabolites found in tissues.[9] Their synthesis depends on the dietary uptake of essential precursors, such as linoleic acid (18:2ω6) and α-linolenic acid (18:3ω3). These precursors are rapidly converted, mainly to AA and DHA, in the gastrointestinal tract and in the liver and are temporarily stored as tissue phospholipids.[10] Moreover, the organ specificity for AA and DHA is different, as is their mode of action in signal transduction processes. The ω3 series is especially important for neural functions in the central nervous system, as shown by dietary-dependent effects on learning[2] and on visual function in animals and in human infants.[1,11,12] One hypothesis is that some of the biological functions of PUFAs are mediated by G protein-coupled receptors such as rhodopsin.[13]

For an understanding of the biological relevance of phospholipid unsaturation, it will ultimately be necessary to gain insight into the physical characteristics of PUFA-containing phospholipid membranes. Several deuterium (^{2}H) NMR studies of DHA-containing lipid bilayer membranes have been previously conducted.[14−18] (For a review of solid-state NMR spectroscopy of biomembranes, see ref 19.) The present study has focused on a comparison of phosphatidylcholines (PC) as a function of increasing unsaturation of the *sn*-2 fatty acyl moiety, as investigated by solid-state ^{2}H NMR spectroscopy and all-atom molecular dynamics (MD) computer simulations. The purpose of this comparison is to utilize the well-known properties of the monounsaturated lipid, 1-palmitoyl-2-oleoyl-*sn*-glycero-3-phosphocholine (POPC), denoted as (16:0)(18:1)-PC, together with state-of-the-art MD simulations of the same system as a framework to explore the features of 1-palmitoyl-2-docosahexaenoyl-*sn*-glycero-3-phosphopholine (PDPC), designated (16:0)(22:6)PC. The structures of both lipids are schematically shown in Figure 1. The validity of the MD simulations was investigated with reference to structural and dynamical information obtained by NMR[7,15] and small-angle X-ray scattering. For bilayers of the polyunsaturated lipid PDPC in the fluid, liquid-crystalline (L_α) state, we show the conformational space accessible to the DHA chain and characterize the preferred structures in relation to previous theoretical work.[20,21] The conformations are analyzed in terms of dihedral angular probability distribution functions, or equivalently the potential of mean force, analogous to Ramachandran plots for polypeptides. In phospholipid bilayers, we found exhaustive sampling of the accessible conformational space for DHA, with a tendency to form rather extended structures, previously described as helical and angle-iron conformations.[20,21] The presence of relatively long, extensible fatty acyl chains may be important for solvating the hydrophobic surface of rhodopsin, as evident in the X-ray crystal structure.[22] As a rule, these findings provide a conceptual basis for interpretation of the influences of polyunsaturated lipids on biological functions at the molecular level.

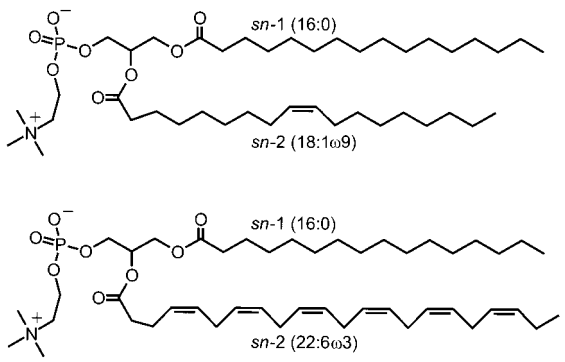

Figure 1. Structures of the monounsaturated phospholipid 1-palmitoyl-2-oleoyl-*sn*-glycero-3-phosphocholine (POPC) and the polyunsaturated phospholipid 1-palmitoyl-2-docosahexaenoyl-*sn*-glycero-3-phosphocholine (PDPC).

Experimental and Theoretical Procedures

Synthesis of Phospholipids and Sample Preparation. The lipids studied were *sn*-1 chain perdeuterated POPC-d_{31}, 1-perdeuteriopalmitoyl-2-oleoyl-*sn*-glycero-3-phosphocholine, obtained from Avanti Polar Lipids (Alabaster, AL), and POPC-d_9, 1-palmitoyl-2-oleoyl-*sn*-glycero-3-trideuteriomethyl-phosphocholine, which was synthesized from 1-palmitoyl-2-oleoyl-*sn*-glycero-3-phosphoethanolamine.[23] In addition, the *sn*-1 chain perdeuterated PDPC-d_{31}, 1-perdeuteriopalmitoyl-2-docosahexaenoyl-*sn*-glycero-3-phosphocholine, and the *sn*-2 chain deuterated PDPC-d_{12}, 1-palmitoyl-2-vinylperdeuteriodocosahexaenoyl-*sn*-glycero-3-phosphocholine, were synthesized as described for arachidonic acid-containing phosphatidylcholines.[15,24] Very briefly, the hexaacetylene precursor of DHA, docosahexaynoic acid, was first esterified with methanol in the presence of boron trifluoride etherate and then hydrogenated with deuterium gas in perdeuterated methanol using Lindlar catalyst in the presence of quinoline. The raw product was purified and converted to the free acid. The vinyl perdeuterated docosahexaenoic acid was used to synthesize PDPC-d_{12} by acylation of 1-palmitoyl-*sn*-glycero-3-phosphocholine, the corresponding lysophospholipid, in dimethylfor-

(3) Youdim, K. A.; Martin, A.; Joseph, J. A. *Int. J. Dev. Neurosci.* **2000**, *18*, 383−399.
(4) Stillwell, W. *Curr. Org. Chem.* **2000**, *4*, 1169−1183.
(5) Siddiqui, R. A.; Jenski, L. J.; Neff, K.; Harvey, K.; Kovacs, R. J.; Stillwell, W. *Biochim. Biophys. Acta* **2001**, *1499*, 265−275.
(6) Freedman, S. D.; Katz, M. H.; Parker, E. M.; Laposata, M.; Urman, M. Y.; Alvarez, J. G. *Proc. Natl. Acad. Sci. U.S.A.* **1999**, *96*, 13995−14000.
(7) Dratz, E. A.; Deese, A. J. In *Health Effects of Polyunsaturated Fatty Acids in Seafoods*; Simopoulos, A. P., Kifer, R. R., Martin, R. E., Eds.; Academic Press: New York, 1986; pp 379−412 and references therein.
(8) Yuan, C.; Chen, H. M.; Anderson, R. E.; Kuwata, O.; Ebrey, T. G. *Comp. Biochem. Physiol., B* **1998**, *120*, 785−789.
(9) Crawford, M. A.; Bloom, M.; Broadhurst, C. L.; Schmidt, W. F.; Cunnane, S. C.; Galli, C.; Gehbremeskel, K.; Linseisen, F.; Lloyd-Smith, J.; Parkington, J. *Lipids* **1999**, *34*, S39−S47.
(10) Nilsson, A.; Becker, W. *Am. J. Physiol.* **1995**, *31*, G732−G738.
(11) Salem, N.; Niebylski, C. D. *Mol. Membr. Biol.* **1995**, *12*, 131−134.
(12) Hoffman, D. R.; Birch, E. E.; Birch, D. G.; Uauy, R.; Castaneda, Y. S.; Lapus, M. G.; Wheaton, D. H. *J. Pediatr. Gastroenterol. Nutr.* **2000**, *31*, 540−553.
(13) Brown, M. F. *Curr. Top. Membr.* **1997**, *44*, 285−356.
(14) Paddy, M. R.; Dahlquist, F. W.; Dratz, E. A.; Deese, A. J. *Biochemistry* **1985**, *24*, 5988−5995.
(15) Salmon, A.; Dodd, S. W.; Williams, G. D.; Beach, J. M.; Brown, M. F. *J. Am. Chem. Soc.* **1987**, *109*, 2600−2609.
(16) Barry, J. A.; Trouard, T. P.; Salmon, A.; Brown, M. F. *Biochemistry* **1991**, *30*, 8386−8394.
(17) Holte, L. L.; Peter, S. A.; Sinnwell, T. M.; Gawrisch, K. *Biophys. J.* **1995**, *68*, 2396−2403.
(18) Petrache, H. I.; Salmon, A.; Brown, M. F. *J. Am. Chem. Soc.* **2001**, in press.
(19) Brown, M. F. In *Biological Membranes*; Merz, K. M., Jr., Roux, B., Eds.; Birkhäuser: Boston, 1996; pp 175−252.
(20) Applegate, K. R.; Glomset, J. A. *J. Lipid Res.* **1986**, *27*, 658−680.
(21) Applegate, K. R.; Glomset, J. A. *J. Lipid Res.* **1991**, *32*, 1635−1644.
(22) Palczewski, K.; Kumasaka, T.; Hori, T.; Behnke, C. A.; Motoshima, H.; Fox, B. A.; Le Trong, I.; Teller, D. C.; Okada, T.; Stenkamp, R. E.; Yamamoto, M.; Miyano, M. *Science* **2000**, *289*, 739−745.
(23) Sixl, F.; Watts, A. *Biochemistry* **1982**, *21*, 6446−6452.
(24) Rajamoorthi, K.; Brown, M. F. *Biochemistry* **1991**, *30*, 4204−4212.

mamide, in the presence of 1,3-dicyclohexylcarbodiimide, 4-hydroxybenzotriazole, and 4-pyrrolidinopyridine. The *sn*-1 chain perdeuterated PDPC-d_{31} was synthesized by acylation of 1-perdeuteriopalmitoyl-*sn*-glycero-3-phosphocholine with DHA. The resulting phospholipids were purified by silica gel column chromatography.

The POPC bilayers comprising 15−30 mg of lipid were prepared as macroscopically oriented membranes on 50 ultrathin glass plates (8 × 18 × 0.08 mm; Marienfeld Laboratory Glassware, Bad Mergentheim, Germany), as described,[25] and measured at variable temperature between 25 and 50 °C and variable hydration with ^2H_2O, ranging from about 4 to 25 waters per lipid. ^{31}P NMR spectra were recorded at 27 °C with an interlamellar hydration of 24.3 water molecules per lipid. The PDPC experiments were performed using approximately 200−250 mg of either PDPC-d_{31} or PDPC-d_{12}, dispersed in an equal weight of 67 mM sodium phosphate buffer, pH 7.0, prepared from ^2H-depleted ^1H_2O (Aldrich, WI), containing 10^{-4} M EDTA and 0.01 wt % NaN_3. All samples were checked after the NMR experiments by thin-layer chromatography and revealed no contamination or degradation.

Solid-State NMR Spectroscopy. All POPC experiments were performed on a Varian VXR400S spectrometer equipped with a high radio frequency power amplifier and a solid-state NMR probe with a transverse 10 mm coil at a magnetic field strength of 9.4 T, as described elsewhere.[25] Deuterium NMR spectroscopy of the multilamellar lipid dispersions at either 7.06 or 8.48 T used the solid quadrupolar echo, with the sequence $(\pi/2)_x$-τ-$(\pi/2)_y$-τ-acquire, followed by Fourier transformation. A home-built ^2H NMR probe was used, having a horizontal solenoidal radio frequency coil design, together with high-voltage capacitors (Polyflon, Norwalk, CT). A kilowatt radio frequency boost amplifier (Model Tempo 2006, Henry Radio, Los Angeles, CA) was used in series with the spectrometer output to enable 90° pulse durations <3−4 μs for the 10 mm radio frequency coil. Typical spectral acquisition parameters involved a pulse spacing (τ) of 40 μs, a dwell time of 2 μs (spectral width of ±250 kHz), and collection of 2048 data points. Recycle times were generally 1 s, and typically 600−2400 transients were collected, apodized by exponential multiplication (100 Hz line broadening), and Fourier transformed beginning at the maximum of the solid echo. Both quadrature channels were used, and the spectra were not symmetrized. The sample temperature was monitored before and after each measurement with a thermistor inserted directly above the radio frequency coil and was usually found to vary by less than 0.5 °C during a given run. The temperatures are estimated accurate to within ±1 °C of the reported values.

Data Analysis and Reduction. Powder-type ^2H NMR spectra of the multilamellar dispersions of PDPC-d_{31} and PDPC-d_{12} were numerically deconvoluted (de-Paked), as previously described.[15,19] The deconvoluted spectra correspond to an orientation $\theta = 0°$ of the bilayer normal with respect to the magnetic field. Likewise, macroscopically aligned bilayers of POPC-d_{31} and POPC-d_9 were oriented in the magnetic field with $\theta = 0°$. The quadrupolar splittings were determined directly from the symmetry-related signals of the quadrupolar doublets. The number of deuterons generating a peak is assumed proportional to the area under each peak.[26] The quadrupolar splittings of the partially overlapping lines in the plateau region of PDPC-d_{31} were resolved by fitting them to seven Gaussian functions with equal area. The C−^2H segmental order parameters were calculated from the observed quadrupolar splittings, using a static quadrupolar coupling constant of 170 kHz for the aliphatic C−^2H bonds[19] and 175.3 kHz for the olefinic C−^2H bonds.[27] The analysis of the order parameter profiles of perdeuterated acyl chains does not allow for unambiguous assignment of order parameters to the actual segmental position in the acyl chain, as in the case of a specifically labeled segment. A generally accepted method for perdeuterated chains is to plot the absolute values of the order parameters in decreasing order, starting with the α-methylene segment C_2 up to the terminal methyl group. The assignments were made in reversed order from the methyl terminus toward the plateau region. Order parameters for the *sn*-1 chain of PDPC-d_{31} at 37 °C were obtained from linear interpolation of the experimental values at 30 and 50 °C. The order parameter profiles for POPC-d_{31} were acquired for a series of different hydration levels at temperatures of 25 and 37 °C and were fitted to an empirical model to get an estimate for the full hydration limit. The order parameter profile for 27 °C was obtained from the full hydration results by linear interpolation in the experimental temperature range.

Modeling and Computational Aspects. All MD simulations were performed using the program NAMD2.[28] The necessary structure topology files were created with the modeling software CHARMM27.[29] Molecular models were qualitatively characterized by the visualization software VMD1.6.[30] The trajectories were quantitatively analyzed using the program package MOLGEOM6, which represents a collection of tools including procedures to calculate segmental volumes by the Voronoi cell method,[31] group density profiles, dihedral angle probability distributions, orientational order parameters, bond vector autocorrelation functions, and NMR relaxation rates from autocorrelation functions.[32] The initial model of the PDPC bilayer was generated by homology modeling, starting from a previous POPC bilayer model.[33] A structural model of DHA was built by molecular modeling and was used as input for the distance geometry program DGEOM95,[34] with the necessary information on the covalent geometry. Knowledge of the bond lengths and angles was used together with torsion angle constraints for the double bonds to set up the distance matrix. To replace the oleic acid *sn*-2 chain in the POPC bilayer with DHA, it was necessary to generate DHA conformations with a space-filling shape resembling oleic acid as much as possible. Since the estimated volumes of oleic acid and DHA differ by only about 10%, the oleic acid segment positions were used in the distance geometry program as a template. Equivalent segments of the DHA chain were restrained to match the template positions with a tolerance of 3 Å, except for the first three segments, where the tolerance was 0.5 Å. The DHA conformations generated by the spatial embedding procedure of the distance geometry program were used to replace the oleic acid fragments of the POPC model bilayer. The resulting PDPC bilayer structure was relaxed by conjugate-gradient energy minimization using CHARMM27. Our initial work was based on a modified force field parameter set, which was incorporated into CHARMM27 for lipids.[35] At that time, no parameters were available for a polyunsaturated chain such as DHA. Therefore, we created a set of parameters by fitting an ab initio, quantum-mechanically derived potential energy function for 1,4-pentadiene. However, for all the production work, we used a prerelease version of the force field parameters for lipids with polyunsaturated acyl chains from the developer (CHARMM27b5f) (A. MacKerell, personal communication). The force field parameters from our potential were quite similar to the CHARMM27b5f parameters, which were calculated from 1,4-pentadiene, as in our work, but included also 2,7-heptadiene conformations. We combined the CHARMM27b5f parameter set with the F3C water model.[36] The F3C water model is a fully flexible three-atom model, which was

(25) Kurze, V.; Steinbauer, B.; Huber, T.; Beyer, K. *Biophys. J.* **2000**, *78*, 2441−2451.
(26) Williams, G. D.; Beach, J. M.; Dodd, S. W.; Brown, M. F. *J. Am. Chem. Soc.* **1985**, *107*, 6868−6873.
(27) Kowalewski, J.; Lindblom, T.; Vestin, R.; Drakenberg, T. *Mol. Phys.* **1976**, *31*, 1669−1676.
(28) Kale, L.; Skeel, R.; Bhandarkar, M.; Brunner, R.; Gursoy, A.; Krawetz, N.; Phillips, J.; Shinozaki, A.; Varadarajan, K.; Schulten, K. *J. Comput. Phys.* **1999**, *151*, 283−312.
(29) Brooks, B. R.; Bruccoleri, R. E.; Olafson, B. D.; States, D. J.; Swaminathan, S.; Karplus, M. *J. Comput. Chem.* **1983**, *4*, 187−217.
(30) Humphrey, W.; Dalke, A.; Schulten, K. *J. Mol. Graphics* **1996**, *14*, 33−38.
(31) Goede, A.; Preissner, R.; Frommel, C. *J. Comput. Chem.* **1997**, *18*, 1113−1123.
(32) Pastor, R. W.; Venable, R. M.; Karplus, M.; Szabo, A. *J. Chem. Phys.* **1988**, *89*, 1128−1140.
(33) Huber, T. Ph.D. Dissertation, University of Munich, Munich, Germany, 1999.
(34) Blaney, J. M.; Crippen, G. M.; Dearing, A.; Dixon, J. S.; Spellmeyer, D. C. Quantum Chemical Program Exchange, 1995.
(35) Feller, S. E.; MacKerell, A. D. *J. Phys. Chem. B* **2000**, *104*, 7510−7515.

used instead of one of the usual rigid water models such as TIP3P[37] or SPC/E.[38] The thermodynamic, kinetic, and structural properties of the F3C water model are superior to both TIP3P and SPC/E;[36] further, it allows for a fully flexible all-atom model of the whole system.

MD calculations were performed using a triple time step integration scheme, with the reversible reference system propagator algorithm (*r*-RESPA).[39] Bonded interactions were evaluated every 1 fs, using the F3C and CHARMM potential energy functions. The nonbonded energy, with a 1−4 nonbonded interaction scaling factor of 1.0, was switched by a C1 continuous switching function from 8 Å to the cutoff of 10 Å;[35] that is, the partial derivatives were continuous. To account for the long-range nature of the electrostatic interactions, a full electrostatic calculation was performed. This was done with the distributed particle mesh Ewald method[40] using a 3-D fast Fourier transform cell grid of dimensions 64 × 64 × 64, with less than a 1 Å grid spacing, and a particle mesh Ewald direct space tolerance of 10^{-6} having a cubic interpolation function for grid charges. The nonbonded forces and direct space Ewald sum were evaluated every 2 fs, and the reciprocal space sum was evaluated every 4 fs. A special distance-testing algorithm of the NAMD2.2 program was used with a formal pairlist distance of 1.1 nm and an update period of 24 fs.

The systems modeled in the simulations were oriented multibilayer stacks of the two lipids near full hydration in the liquid-crystalline phase. The PDPC bilayers were simulated at the physiological temperature of 37 °C. The temperature of the POPC bilayers was 27 °C, because of the amount of available literature data close to that temperature. Simulations were performed under periodic boundary conditions, with a flexible orthorhombic simulation cell. A constant particle number, constant pressure, constant surface tension, and constant temperature ($NP\gamma T$) ensemble was generated by an extended system method. The pressure algorithm followed the Nosé-Hoover Langevin piston method, with group pressure scaling, a target pressure of 1.0 bar, and target surface tensions of 20, 45, or 70 mN m^{-1} for the bilayer, that is, a surface tension per interface of 10, 22.5, or 35 mN m^{-1}. The Langevin dynamics parameters for the thermostat algorithm were target temperatures of 37 °C for PDPC and 27 °C for POPC, with period and decay time scales of 1.0 ps for the piston and a damping time constant of 1.0 ps^{-1}. In addition, for some of the simulations the velocities were reassigned according to a Maxwell distribution for the target temperature every 50 ps.

Calculations were performed on a BEOWULF cluster of personal computer workstations using the LINUX operating system. It was possible to obtain approximately 25 ps trajectories per day on each machine for the multiple time step scheme described above. The bilayers used in this study had a size of 72 lipids (36 for each monolayer) and a hydration of 25.4 waters per lipid, yielding a total number of about 15 000 atoms. This water-to-lipid ratio is close to full hydration, as indicated by our results for the hydration dependency of the *sn*-1 acyl chain order parameters of POPC, which showed very low variation beyond about 18 waters per lipid. The starting conformations for POPC were taken from multiple MD simulations. Following a 10 ns MD simulation, six different simulations were run for 1 ns each. The initial velocities for each system were randomly chosen from a Maxwellian distribution, with different random number seeds for every system. This led to different trajectories, each starting from the same structure. The original POPC simulations[33] were performed with different force field parameters and different simulation procedures as compared to the present work. The six POPC systems were simulated for 0.45 ns. The starting conformation was taken in the case of PDPC from preequilibration runs over 1.9−2.3 ns. The main difference in these simulations involved constraining the hydrogen atom bonds by the SHAKE algorithm,[41] with no applied surface tension, in a constant particle number, pressure, and temperature (*NPT*) ensemble. The four PDPC systems finally obtained were changed to an area per lipid of 72 $Å^2$, and to a lamellar spacing of 57.6 Å, by scaling the coordinates according to the box dimensions relative to the desired values. The resulting structures were energy minimized and equilibrated in short constant particle number, volume, and temperature (*NVT*) simulations to give the starting structures for the subsequent simulations. The four different starting structures of the PDPC bilayers were used to start a total of twelve simulations, with applied surface tensions of 20, 45, and 70 mN m^{-1} for each starting structure. The simulation lengths ranged from 0.3 to 0.9 ns, with an overall total of 6.0 ns.

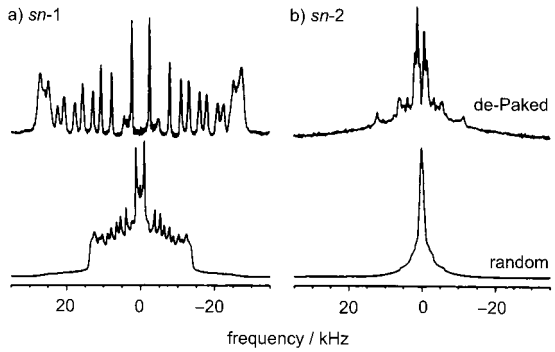

Figure 2. Experimental ^2H NMR spectra of multilamellar dispersions of 1-palmitoyl-2-docosahexaenoyl-*sn*-glycero-3-phosphocholine (PDPC) in the liquid-crystalline (L_α) state. (a) PDPC-d_{31}, showing de-Paked and powder-type spectra of random dispersions. (b) PDPC-d_{12}, showing de-Paked and powder type spectra. The samples contained 67 mM phosphate buffer (50 wt % H_2O), and the ^2H NMR spectra were obtained at 46.13 MHz and 30 °C.

Results

Deuterium NMR Spectroscopy of Polyunsaturated Lipid Bilayers in the Liquid-Crystalline State. Representative ^2H NMR spectra for the palmitic acyl deuterons of PDPC-d_{31} in the liquid-crystalline (L_α) state are shown in Figure 2a. The PDPC-d_{31} results are in good agreement with earlier reports.[14,15] They are also similar to analogous results for 1-perdeuteriopalmitoyl-2-arachidonyl-*sn*-glycero-3-phosphocholine in the liquid-crystalline state.[24] The influences of arachidonic and docosahexaenoic acyl chains on the *sn*-1 perdeuteriostearic acyl chains in homologous PC bilayers are much the same.[17] By contrast, the *sn*-2 vinyl perdeuterated DHA chain of PDPC-d_{12}, with deuteration at the C═C double bond positions ($\Delta^{4,7,10,13,16,19}$), see Figure 1, gives the ^2H NMR spectrum shown in Figure 2b. A similar spectrum for PDPC-d_{12} without de-Pakeing has been reported.[7] Previous ^2H NMR studies of vinyl perdeuterated arachidonic acid chains in bilayers of 1-palmitoyl-2-vinylperdeuterioarachidonyl-*sn*-glycero-3-phosphocholine in the L_α phase yielded a spectrum[24] resembling the DHA chains of the PDPC-d_{12} bilayers. Note the drastically narrowed ^2H NMR spectrum for the *sn*-2 DHA chain, Figure 2b. The narrowing is not due to motional averaging of the quadrupolar splittings, since a broad well-defined powder pattern is observed for the *sn*-1 palmitoyl chain, Figure 2a. The ^2H NMR spectra of oriented samples of POPC-d_{31} were in agreement with previously published results for the same lipid,[42,43] except that

(36) Levitt, M.; Hirshberg, M.; Sharon, R.; Laidig, K. E.; Daggett, V. *J. Phys. Chem. B* **1997**, *101*, 5051−5061.
(37) Jorgensen, W. L. *J. Am. Chem. Soc.* **1981**, *103*, 335−340.
(38) Berendsen, H. J. C.; Grigera, J. R.; Straatsma, T. P. *J. Phys. Chem.* **1987**, *91*, 6269−6271.
(39) Martyna, G. J.; Tuckerman, M. E.; Tobias, D. J.; Klein, M. L. *Mol. Phys.* **1996**, *87*, 1117−1157.
(40) Darden, T.; York, D.; Pedersen, L. *J. Chem. Phys.* **1993**, *98*, 10089−10092.
(41) Ryckaert, J. P.; Ciccotti, G.; Berendsen, H. J. C. *J. Comput. Phys.* **1977**, *23*, 327−341.

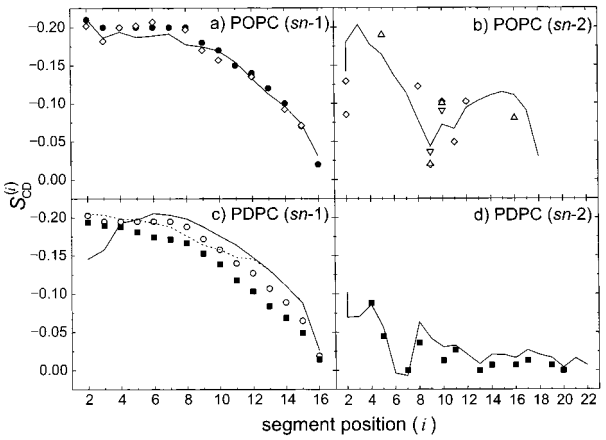

Figure 3. Experimental and simulated C−^{2}H chain segmental order parameters (S_{CD}) for monounsaturated and polyunsaturated phosphatidylcholines in the L_α phase. (a) POPC, *sn*-1 palmitoyl (16:0) acyl chain; (◇) S_{CD} data for selectively deuterated POPC at 27 °C taken from ref 45; (●) S_{CD} data for POPC-d_{31} at 27 °C; (—) S_{CD} calculated from the MD trajectory at 27 °C. (b) POPC, *sn*-2 acyl chain; (◇) S_{CD} data for selectively deuterated POPC at 27 °C taken from ref 46; (△) S_{CD} data for selectively deuterated POPC at 30 °C taken from ref 77; (▽) S_{CH} data for egg PC at unspecified temperature taken from ref 78; (—) S_{CD} calculated from the MD trajectory at 27 °C. (c) PDPC, *sn*-1 palmitoyl acyl chain; (■) S_{CD} data for PDPC-d_{31} linearly interpolated to 37 °C from data at 30 °C and 50 °C; (○) S_{CD} data for POPC-d_{31} at 37 °C; (—) S_{CD} calculated from the MD trajectory at 37 °C; (- - -) S_{CD} calculated from the MD trajectory at 37 °C, but sorted to decrease along the chain in comparison with the experimental values. (d) PDPC, *sn*-2 docosahexaenoyl (C22:6ω3) acyl chain; (■) S_{CD} data for PDPC-d_{12} at 30 °C, experimental order parameters assigned to individual segments by comparison to simulated order parameters; (—) S_{CD} calculated from the MD trajectory at 37 °C.

our studies used deuterated water for simultaneous determination of the number of oriented waters per lipid and the hydration dependency of the order parameter profile (not shown).

Order Parameters of Unsaturated and Polyunsaturated Phosphatidylcholines. The average structures of lipids in the liquid-crystalline state can be described in terms of orientational order parameters, as discussed by Petrache et al.[44] The order matrix ***S*** has the diagonal elements

$$S_{ii} = \frac{1}{2}\langle 3\cos^2\beta_{ii} - 1\rangle \qquad (1)$$

where $i = x, y, z$. In the case of ^{2}H NMR, cos β_{ii} represents the direction cosines between the Cartesian principal axes of the coupling tensor and the director axis, perpendicular to the bilayer surface. The brackets $\langle\ \rangle$ denote an ensemble and/or time average. The C−^{2}H bond order parameters correspond to S_{zz}, with the largest principal value of the coupling tensor oriented along the bond direction and the director axis oriented along the bilayer *z* coordinate. The average structure of the bilayer can be described in terms of segmental order parameter profiles for the phospholipid acyl chains. The segmental C−^{2}H bond order parameters, S_{CD}, for the *sn*-1 and *sn*-2 chains of POPC and PDPC, as obtained by ^{2}H NMR and by the MD simulations, are summarized in Figure 3. Acyl chain order parameters have been previously obtained for the selectively deuterated palmitoyl and oleoyl acyl chains of POPC in the liquid-crystalline state at 27 °C.[45,46] In addition, we determined order parameter profiles for POPC-d_{31} and PDPC-d_{31} in the L_α phase. The ^{2}H NMR spectra reveal that the packing behaviors of the saturated and polyunsaturated fatty acyl chains of the mixed-chain PDPC bilayer differ significantly. Comparison of the experimental order parameters for POPC with the results based on our MD simulations shows the predictive power of the simulated bilayer model.

Figure 3a and b shows the order parameter profiles for the *sn*-1 palmitoyl and *sn*-2 oleoyl chains of POPC in the liquid-crystalline state. In addition, the experimental order parameter profiles of the *sn*-1 palmitoyl and *sn*-2 DHA chains of PDPC at 37 °C are included in Figure 3c and d. The experimental order parameter profiles for POPC and PDPC with perdeuterated *sn*-1 chains were assigned by assuming monotonically decreasing absolute values, from the beginning of the chain near the aqueous interface to the tail segments. For comparison, the simulated values are plotted versus the segment position as directly calculated from the model. In Figure 3c, the simulated order parameters are also graphed in decreasing order of their absolute values. Note that compared to bilayers of POPC and disaturated phospholipids, there is an increase in disorder toward the end of the saturated *sn*-1 chain, due to the adjacent polyunsaturated DHA chain at the *sn*-2 position.[15] The experimental order parameters of the *sn*-2 DHA chain of PDPC were assigned to specific segments by comparison with the simulated order parameters for the DHA chain. A direct comparison of the profiles obtained for POPC-d_{31} and PDPC-d_{31} by ^{2}H NMR at 37 °C for the *sn*-1 chains is also included in Figure 3c. The transition temperatures T_m for fully hydrated bilayer membranes of POPC-d_{31} and PDPC-d_{31} are −6 °C[47] and −3.0 °C, respectively, with a hysteresis of 9.7 °C for the latter;[16] that is, the relative temperatures ($T - T_m$) are very close at 37 °C. It can be seen that the order parameters, assigned to carbon positions C_2−C_4 and C_{16}, are very similar for these lipids, whereas significantly different order parameters are found for positions C_5−C_{15}. Thus, the concept of reduced temperature may not account entirely for thermal influences in lipid systems having different acyl chains at the glycerol *sn*-2 position.[16]

Molecular Dynamics Simulations of Unsaturated and Polyunsaturated Phosphatidylcholines. The energy evaluation scheme, especially the details concerning nonbonded energies, follows ref 35. Compared to prior work,[48] in which the dependence of the DPPC area per lipid on the surface tension of the bilayer cell was evaluated, here we have used a different version of the force field, viz. CHARMM27b5f as compared to CHARMM22b4b, and a different approximation for the Lennard-Jones potential, with a smooth switching to zero interaction energy between 8 and 10 Å versus 10−12 Å. In the present work, all bonds were treated as flexible, and a time step of 1 fs was used to integrate over the fastest dynamical modes. The fully flexible water model F3C[36] was added to the force field parameter set. With respect to ref 35, where SHAKE[41] was used to constrain all covalent bonds involving hydrogens and an integration time step of 2 fs, the shorter time step in our simulation, without losses in computational performance, was possible due to use of a multiple time-stepping *r*-RESPA

(42) Lafleur, M.; Fine, B.; Sternin, E.; Cullis, P. R.; Bloom, M. *Biophys. J.* **1989**, *56*, 1037−1041.
(43) Morrison, C.; Bloom, M. *J. Chem. Phys.* **1994**, *101*, 749−763.
(44) Petrache, H. I.; Dodd, S. W.; Brown, M. F. *Biophys. J.* **2000**, *79*, 3172−3192.
(45) Seelig, A.; Seelig, J. *Biochemistry* **1977**, *16*, 45−50.
(46) Seelig, J.; Waespe-Šarčević, N. *Biochemistry* **1978**, *17*, 3310−3315.
(47) Lafleur, M.; Cullis, P. R.; Bloom, M. *Eur. Biophys. J.* **1990**, *19*, 55−62.
(48) Feller, S. E.; Pastor, R. W. *J. Chem. Phys.* **1999**, *111*, 1281−1287.

integration.[39] The idea behind this modification was to address the problem of temperature differences between the solute and solvent subsystems.[49] The differences were generally smaller when temperature and pressure were controlled with extended system methods, as in the present work, versus use of a weak coupling algorithm.[50] Compared to SHAKE, a further reduction of the temperature mismatch was possible using the multiple time-stepping *r*-RESPA method.[49] The choice of the different time steps of 1 fs for the bonded interactions, 2 fs for the nonbonded interactions and the direct space part of the Ewald sum, and 4 fs for the reciprocal space part of the Ewald sum was supported by dynamics stability tests.[36]

The properties of the simulations of the polyunsaturated bilayers were explored in some preproduction simulations, which were not included in the structural analysis presented here. A *NVT* simulation of the PDPC bilayer at a constant surface area of 72 Å^2 per lipid at 37 °C was more consistent with the experimental S_{CD} order parameter profile than the exploratory *NPT* simulations, where the average area per lipid was about 65.8 Å^2. These simulations were performed at target temperatures of 27, 37, and 50 °C, with a 2 fs time step, with use of SHAKE[41] for hydrogen atom bond length constraints. Interestingly, without an applied surface tension the simulations paradoxically[51] resulted in a decrease in the area per lipid with increasing temperature. Moreover, the absolute values of the order parameter profile for the *sn*-1 chain were found to be too high compared with the actual experimental data, indicating a smaller area per lipid in comparison to that of the real system. Such a behavior, also reported by other groups,[52] is interpreted as an influence of the finite size of the system.[53] The finite size of the simulation cell under periodic boundary conditions as compared to a large membrane, having additional degrees of freedom, possibly involving undulations,[54] leads to a reduction of the surface pressure in the membrane. This surface pressure is balanced by the effective surface tension resulting in a stress-free state of the bilayer. Any reduction in the surface pressure, for example, through finite size effects, leads to a reduction in surface area until the surface pressure increases enough to balance the surface tension. To compensate for this finite size effect, a nonzero additional surface tension should be applied to the system.[48] The production work simulations for bilayer membranes of POPC at 27 °C and of PDPC at 37 °C were thus performed with applied surface tensions of 20, 45 (PDPC only), and 70 mN m^{-1}.

The equilibrium values of the area per lipid for different values of the surface tension can also be used to estimate the membrane lateral compressibility at constant temperature, viz. in terms of the area elastic modulus K_a, by the relation:[54]

$$K_a = A\left(\frac{\partial \gamma}{\partial A}\right)_T \qquad (2)$$

Here γ is the applied surface tension, and A is the area per lipid. The value of K_a was calculated from the dependence of the surface tension values on the area per lipid (direct method). The simulations at bilayer surface tension values of 20, 45, and 70 mN m^{-1} resulted in a value of $K_a = 0.38$ J m^{-2}, which can be compared to the value of 0.34 J m^{-2} for PDPC obtained by a different approach.[55] Bilayers of disaturated PC lipids in the liquid-crystalline phase have smaller values for K_a, as obtained from MD[48,54] and statistical thermodynamic calculations.[55] The conclusion is that the introduction of a polyunsaturated acyl chain can lead to a modest decrease of bilayer elasticity.

Order Parameters from Simulated Ensembles: Comparison to Experimental Results. The quality of the MD-generated ensemble for POPC can be seen from the standard deviation of the difference of the experimental order parameters and those calculated from the MD simulation, which is 0.02 for 27 experimentally available segment positions distributed throughout the entire molecule.[33] The signed order parameters were compared if experimentally determined; the absolute values were compared for the other cases. In addition, the ^{31}P NMR chemical shift anisotropy was calculated and compared with the experimental value (not shown). It is usually assumed that the acyl chain methylene order parameters have a negative value and are indistinguishable for both prochiral deuterons of an individual C^2H_2 segment. However, this is not the case for some segments, for instance, the C_2 position of the *sn*-2 acyl chain. In the case of 1,2-dipalmitoyl-*sn*-glycero-3-phosphocholine (DPPC), it has been determined by stereoselective deuteration that the larger order parameter of the two splittings corresponds to the pro-*R* position, and the smaller corresponds to the pro-*S* deuteron.[56] From the size of the corresponding splitting in POPC as compared to that in DPPC and their temperature dependencies,[57] one can conclude that the stereoselective assignment is also applicable to POPC. The ^{2}H NMR order parameters of the olefinic ($-C^2H{=}C^2H-$) deuterons of POPC have also been determined.[46]

With regard to the polyunsaturated PDPC bilayer, appreciably less experimental data are available than for the case of POPC. Compared to the POPC bilayer, the S_{CD} order profiles for the *sn*-1 palmitoyl chain of PDPC-d_{31} show a *decrease* in configurational order near their end, viz. close to the bilayer center (vide supra). Qualitatively, the increased disorder near the end of the saturated *sn*-1 chains of the mixed-chain PDPC bilayers can be explained by the influence of bent (hairpin-like) conformers of the DHA chain. By contrast, the extended conformers (helix, angle-iron) would be expected to *increase* the acyl chain ordering in the central bilayer region. As can be seen in Figure 3c, for PDPC the ^{2}H NMR-derived order parameters for the *sn*-1 chain show significantly higher deviation from the simulated values than in the case of POPC. However, the agreement is already satisfactory at this level of refinement of the MD simulation method. It is noteworthy that our experimental ^{2}H NMR studies of the dehydration of POPC-d_{31} bilayers have demonstrated a characteristic change of the *sn*-1 chain order parameter profile. The initial region of the order parameter profile was less sensitive to dehydration than was the tail region, with the latter having a larger increase in order upon dehydration (not shown). The simulated *sn*-1 order profile for PDPC reveals similar changes as the experimental dehydration effect for POPC. The experimental ^{2}H NMR order

(49) Cheng, A. L.; Merz, K. M. *J. Phys. Chem. B* **1999**, *103*, 5396−5405.
(50) Feller, S. E.; Zhang, Y. H.; Pastor, R. W.; Brooks, B. R. *J. Chem. Phys.* **1995**, *103*, 4613−4621.
(51) Bloom, M.; Evans, E.; Mouritsen, O. G. *Q. Rev. Biophys.* **1991**, *24*, 293−397.
(52) Chiu, S. W.; Clark, M.; Balaji, V.; Subramaniam, S.; Scott, H. L.; Jakobsson, E. *Biophys. J.* **1995**, *69*, 1230−1245.
(53) Feller, S. E.; Pastor, R. W. *Biophys. J.* **1996**, *71*, 1350−1355.
(54) Lindahl, E.; Edholm, O. *J. Chem. Phys.* **2000**, *113*, 3882−3893.
(55) Cantor, R. S. *Biophys. J.* **1999**, *76*, 2625−2639.
(56) Engel, A. K.; Cowburn, D. *FEBS Lett.* **1981**, *126*, 169−171.
(57) Seelig, J.; Seelig, A. *Q. Rev. Biophys.* **1980**, *13*, 19−61.

parameter profile for PDPC shows a reduction for the tail region of the *sn*-1 chain as compared to that of POPC and an even greater difference versus the simulated PDPC profile. It is plausible that the observed difference in chain order of the PDPC bilayers from the MD simulation and the NMR experiment corresponds to a dehydration of the hydrophobic core and vice versa. On the other hand, Figure 3d shows that the distribution of order parameters for the olefinic C−^{2}H bonds of the polyunsaturated *sn*-2 DHA chain are in quite good agreement with the simulated data. As can be seen, the order profile for the *sn*-2 DHA chain of the PDPC-d_{12} bilayer is substantially reduced as compared to that of the *sn*-1 palmitoyl chain. Apart from the overall decrease in absolute magnitude, the slope of the initial part of the DHA order profile involving carbons C_3−C_{10}, Figure 3d, is reminiscent of the region of the POPC order profile in the vicinity of the double bond, comprising carbons C_7−C_{11}, Figure 3b. Beyond C_{10}, the DHA chain order profile becomes increasingly less structured. These observations suggest that the region comprising the first two double bonds of the DHA chain represent the most well-ordered part of the bilayer, with an accumulation of disorder along the polyunsaturated chains toward the bilayer center. The interpretation of the results for the DHA chain is further described below.

Atomic Group Distributions: Comparison to X-ray Electron Density Profiles. Due to the periodicity of multilamellar lipid bilayers along the membrane normal direction, neutron and X-ray scattering methods can be used to study their density distributions. The contribution of the atoms is related to the densities of the scattering particles, for example, the atomic electrons for X-ray scattering and atomic nuclei for neutron scattering. From the MD simulations, these density distributions are available for all atoms separately, and it is convenient to show the distribution functions for the various individual groups (Figure 4). For both the POPC and PDPC bilayers, Figure 4a and b, the upper parts of the figure show the electron density-weighted sums of the lipid and the water parts, which contribute separately to the total electron density profile. In addition, we show the results derived for the individual group distributions along the bilayer normal.

For POPC in the L_α state, it has been shown from small-angle X-ray scattering data that the repeat distance and structure factors are very similar to bilayers of egg PC.[58] Consequently, to compare the simulated electron density profile for POPC with experimental data, we have used the hydration-dependent structure factors for egg PC at 30 °C[59] and at 23 °C.[60] The deviations of the shape of the simulated electron density profile as compared to those of the experimental electron density profiles (not shown) are small, given that the amplitudes of the experimental profiles are scaled to match the simulated profile. The structural interpretation of diffraction experiments for bilayer dispersions has been discussed in an excellent recent review.[61] For fully hydrated egg PC bilayers at 30 °C, it was concluded that the area per lipid is 69.4 ± 1.1 Å^2, and the equilibrium lamellar repeat distance is 66.3 Å.[59] The electron density profile for POPC in Figure 4 was obtained for an ensemble with an area per lipid of 72.2 Å^2 and a lamellar repeat distance of 56.3 Å. The repeat distance depends strongly on hydration up to the equilibrium value. It should be noted that recent results on fully hydrated multilamellar POPC bilayers at 50 °C resulted in an area per lipid of 62 ± 1 Å^2.[62]

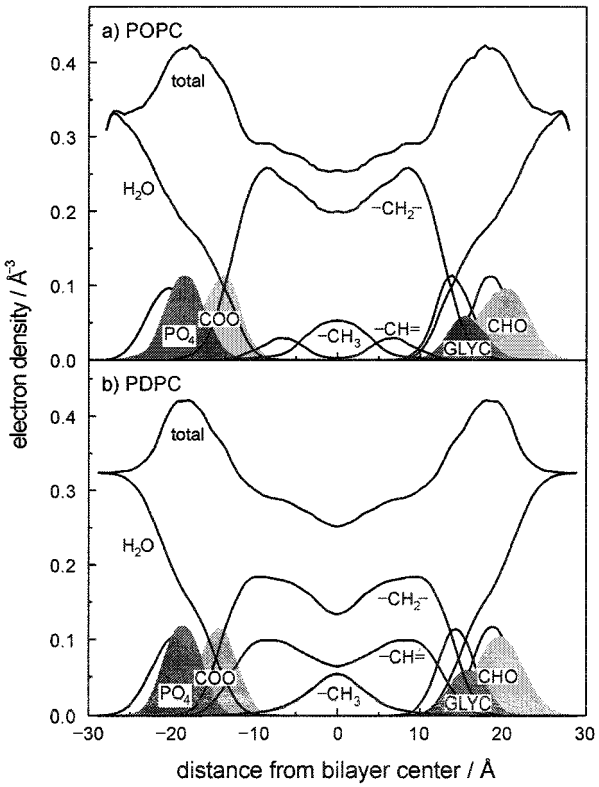

Figure 4. Electron density profiles and segmental group distribution functions. (a) Simulated electron density profile for the POPC bilayer at 27 °C; (b) simulated profile for the PDPC bilayer at 37 °C. The contributions of the lipid segments and water are designated as follows: total corresponds to lipids and water; H_2O, water; CHO, choline group; PO_4, phosphate; GLYC, glycerol; COO, ester carbonyl; CH_2, methylene; CH, vinyl; and CH_3, methyl groups.

In the case of the PDPC bilayer, we have only an experimental electron density profile obtained at 93% relative humidity and 10 °C.[63] The distance between the headgroup peaks across the bilayer is about 35 Å for PDPC. For an ensemble with an average aqueous interfacial area of 70.3 ± 5.9 Å^2, the simulated electron density profile for PDPC at 37 °C showed a distance between headgroup peaks of about 38.2 Å. A second ensemble set with an average area of 77.8 ± 11.8 Å^2 resulted in a headgroup distance of 33.7 Å. The origin for these rather large standard deviations are the multiple trajectories, which do not converge rapidly to a common area per lipid at either of the applied surface tensions of 20 and 70 mN m^{-1}. Since we wish to compare the effect of introduction of the *sn*-2 DHA chain, Figure 4 presents the results for an ensemble of PDPC that is similar to POPC, having an interfacial area per lipid of 72.3 Å^2 and a lamellar repeat distance of 58.3 Å. As can be seen, the distributions of the headgroup segments are virtually identical for POPC and PDPC. The acyl chain region is somewhat broader for PDPC, and the relative contribution of the methylene segments to the hydrocarbon core of the bilayers clearly depends

(58) McIntosh, T. J.; Holloway, P. W. *Biochemistry* **1987**, *26*, 1783−1788.
(59) Petrache, H. I.; Tristram-Nagle, S.; Nagle, J. F. *Chem. Phys. Lipids* **1998**, *95*, 83−94.
(60) McIntosh, T. J.; Simon, S. A. *Biochemistry* **1986**, *25*, 4058−4066.
(61) Nagle, J. F.; Tristram-Nagle, S. *Biochim. Biophys. Acta* **2000**, *1469*, 159−195.
(62) Pabst, G.; Rappolt, M.; Amenitsch, H.; Laggner, P. *Phys. Rev. E* **2000**, *62*, 4000−4009.
(63) Rajamoorthi, K.; McIntosh, T. J.; Barry, J. A.; Trouard, T. P.; Salmon, A.; Brown, M. F., unpublished results.

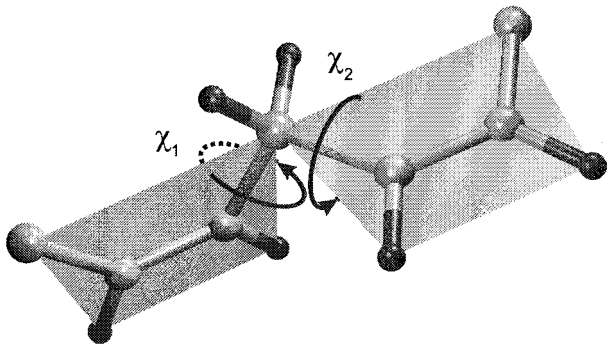

Figure 5. Definition of the dihedral angles χ_1 and χ_2 for a methylene group in a −CH═CH−CH$_2$−CH═CH− acyl fragment. The conformation of the structure shown is $\chi_1 = \chi_2 = 120°$ (skew+, skew+).

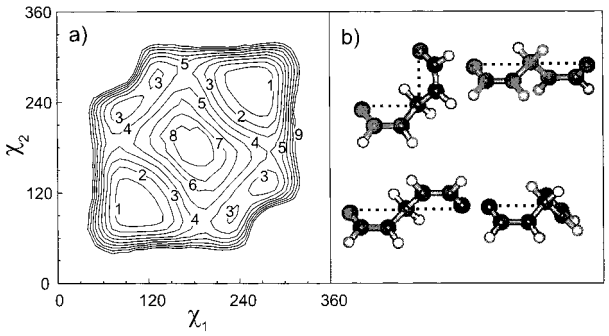

Figure 6. Dihedral angle distribution function, presented in terms of mean force potential, where χ_1 and χ_2 are the two adjacent dihedral angles for the methylene group of a −CH═CH−CH$_2$−CH═CH− fragment. The data are averaged over the trajectories for all five inequivalent positions of the docosahexaenoic acyl chain of PDPC. (a) Contour plot of the potential of mean force calculated from the probability distribution, spanning the (χ_1,χ_2) plane, with a linear spacing of 1 kJ mol^{-1} between contour levels. The levels are labeled by the free energy in kJ mol^{-1} relative to the most probable conformation, which is assigned to the zero level. (b) Conformations corresponding to (χ_1,χ_2) values of (skew+, skew−), (skew−, skew−), (skew+, skew+), and (skew−, skew+). The skew+ conformation corresponds to a dihedral angle of 120°, and the skew− conformation corresponds to a dihedral angle of 240°, that is, −120°.

on the degree of acyl unsaturation. Interestingly, the water density profile shows less penetration into the bilayer for PDPC as compared to that of POPC, which leads to a larger repeat distance at the same area and number of water molecules per lipid. Considering the 4.3% larger volume per lipid for PDPC as compared to that of POPC, as calculated from the MD simulated ensembles, and the comparable area per lipid in both cases, the bilayer thickness for PDPC must be larger, which is reflected in the reduced water penetration into the bilayer, as compared to that of POPC. The slightly larger thickness of the hydrophobic core of the PDPC bilayer, as compared to that of POPC, is an important quantity for the interaction of integral membrane proteins with the lipid matrix.

Conformational Statistics of Docosahexaenoic Acyl Chains. Our choice of the torsion angle conventions followed Hauser et al.[64] The torsional conformations for different values of a dihedral angle are designated as cis (0°), gauche+ (60°), skew+ (120°), trans (180°), skew− (240°), and gauche− (300°), which designate the positions of the two substituents (C atoms) across the single bond (cf. Figure 5). In polyunsaturated fatty acids, such as DHA, pairs of adjacent cis double bonds are separated from one another by a single methylene carbon (double allylic). As can be seen in Figure 1, this double allylic repeating motif constitutes almost the full *sn*-2 acyl chain in PDPC. Due to the rigid nature of the double bond, the vector joining two methylene carbons separated by a double bond is parallel to the double bond itself. In this regard, there is a clear structural analogy to polypeptide structures such as polyglycine,[15] where the planar repetitive units are trans in the case of a normal peptide bond, which has a double bond character. Thus, a Ramachandran-type analysis can be applied to both. It follows that the pair of dihedral angles associated with a doubly allylic methylene carbon (Figure 5) can be used to describe the local conformation of the DHA chain.

For the analysis of the DHA chain conformation from the MD trajectory, torsion angles in the range of 0° to 180° are assigned to (+), and torsion angles in the range of −180° to 0°, that is, 180° to 360°, are assigned to (−). In terms of a rotational isomeric state approximation, these conformations were modeled with skew+ and skew− conformations for the torsion angles, here denoted as (+) and (−) for simplicity. We denote these conformations for a doubly allylic methylene carbon as (±,±) for skew±, skew±, and (±,∓) for skew±, skew∓, where the skew conformations correspond to the potential energy optima from a Ramachandran-type analysis (vide infra). Note that if one describes the possible conformations of the entire DHA chain by the torsion angle pairs at the five doubly allylic methylene segments, that is, between the six double bonds, then a total of $2^5 \times 2^5 = 1024$ principal conformers have to be considered, distinguishing just the (+) and (−) values for each dihedral angle. From our analysis of the MD-generated ensemble, involving over 400 000 conformational snapshots of the PDPC molecule, we found allowed structures for all these conformations. This indicates that steric hindrance (cf. Figure 5) does not yield exclusion of conformers at this level of angular resolution, although it leads to the observed large differences of up to three orders of magnitude in the populations of individual conformations. Since the visualization of such a large number of conformations would be quite complex, we reduced the analysis to triene fragments containing three double bonds and two pairs of associated methylene segment torsion angles. By considering only one-half of the conformations, each representing one of the two possible mirror image conformers for each conformation, the 16 principal conformers for a given triene fragment can be further reduced to only eight. A mirror image of a specific conformer is defined by torsion angles of changed sign for all dihedrals; for example, the conformation (−,−)(+,−) has the mirror image (+,+)(−,+), here denoted by (∓,∓)(±,∓). Previous molecular modeling studies of the conformations of DHA have defined a nomenclature for some conformations, that is, the helical (±,±)(±,±), the angle-iron (±,±)(∓,∓), and hairpin (±,∓)(±,∓) and (±,∓)(∓,±) conformations for triene fragments of the chain.[20]

Figure 6 shows the dihedral angle distribution functions, visualized as the potential of mean force, for the two C−C bonds of a doubly allylic methylene carbon averaged over the entire DHA chain. The dihedral angle distributions for each of the five individual diene fragments along the DHA chain have also been computed (not shown). A small increase of the population of the bent conformers relative to the extended conformers is

(64) Hauser, H.; Pascher, I.; Pearson, R. H.; Sundell, S. *Biochim. Biophys. Acta* **1981**, *650*, 21−51.

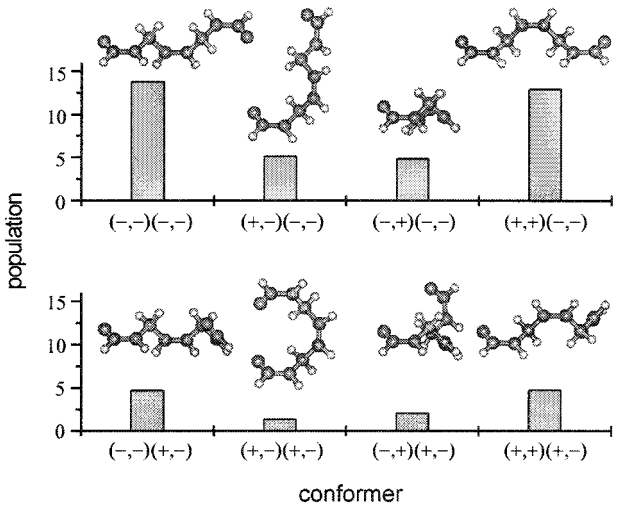

Figure 7. Probabilities for different conformations of triene sequences of the docosahexaenoic acyl chain of PDPC. The conformations correspond to (χ_1,χ_2) and (χ_3,χ_4) for the two methylene groups in a −CH═CH−CH_2−CH═CH−CH_2−CH═CH− fragment, where (+) refers to a dihedral angle in the range from 0° to 180°, and (−) refers to a dihedral angle in the range from −180° to 0°. Note that only one of the two possible mirror images for each conformation is shown for clarity. The population for each conformation is calculated from the average for the two mirror images. The mirror image of one conformation has the same absolute value, but opposite signs for all torsion angles. Differences in the populations of corresponding mirror image conformations were not statistically significant. The populations change by about 10% as the triene sequence is shifted along the chain, with a decrease in the extended conformations and an increase in all the bent-like conformations.

evident along the chain, with little difference in the populations of the corresponding mirror image conformations. As a result, we have chosen to depict the average of the whole DHA chain, which gives a clear picture of the shape of the underlying energy hypersurface. The probability maxima in Figure 6a correspond to the molecular structures shown in Figure 6b. Clearly, the (±,±) conformations, which represent the most probable structures from the simulations, show an extended arrangement of the three methylene carbons attached to the two neighboring double bonds. The (±,∓) conformations, on the other hand, have an almost perpendicular angle between the vector joining the first and second methylene carbon and the vector from the second to the third methylene carbon. We call these conformations, therefore, as bent in contrast to the former extended conformations (vide supra). In terms of the triene fragments of the DHA chain, for the helical conformation (±,±)(±,±), both torsion angle pairs correspond to the same minimum in Figure 6a, whereas for the angle-iron conformer (±,±)(∓,∓), the adjacent torsion angle pairs correspond to opposite minima. The other conformers are mixtures of bent and extended conformations.

In Figure 7, the populations of these triene fragments of the DHA chain obtained from the MD ensemble are shown, together with the molecular structures for each conformer. Note that the populations are statistically equal for the corresponding mirror image conformations, which are not displayed in Figure 7 for clarity. It can be seen that the most populated conformers, together with their implicit mirror image conformations, correspond to an extended arrangement of four methylene carbons joined by the three consecutive double bonds. The four possible extended conformations, viz. the helical (±,±)(±,±) and angle-iron (±,±)(∓,∓) conformers, contribute to about 54% of all conformations at a particular double allylic methylene segment. Eight conformations with one bent configuration (±,∓) and one extended configuration (±,±) contribute to about 39% of all conformations. The remaining conformers have a sequence of two bent conformations, (±,∓)(±,∓) and (±,∓)(∓,±), which lead to hairpin-like turn structures. The three double bonds of the conformations (±,∓)(∓,±) are pairwise orthogonal, whereas in the (±,∓)(±,∓) structure the bond vectors of the first and third double bond are antiparallel. These conformations have the lowest probability. As noted above for the diene fragments, in the case of the triene fragments there is only a small dependence of the population pattern on the position in the entire DHA chain. The extended conformations, that is, the helical and the angle-iron conformers, become less populated at the end of the chain as compared to the beginning, whereas the probability for bent conformations continuously increases (not shown).

Analysis of the entire DHA chain conformation, in term of the ten allylic dihedral angles, displayed exhaustive sampling of the conformational space of the C19:6 substructure. The conformational statistics of the entire DHA chain can be described in terms of the probabilities of bent-like conformations involving the five doubly allylic methylene segments. We calculated the probabilities for zero to five bent-like conformations to be 22.1, 37.5, 27.5, 10.4, 2.30, and 0.17%, respectively. Here, the value for zero bent-like conformations represents the total for all chains with only helical or angle-iron conformations or mixtures of both. Consequently, although the angle-iron and helix structures for the *entire* DHA chain[20] are among the most probable conformations, in the L_α state they contribute only a few percent to all structures! In addition, we have noted previously[15] that helical conformers of variable pitch (helical springs) are possible. The two extremes of helical conformations of DHA are (±,±)(±,±)(±,±)(±,±)(±,±), with a probability of 1.6%, and (±,∓)(±,∓)(±,∓)(±,∓)(±,∓), which is found in only 0.004% of all chains. The latter helical conformation represents an extreme conformation, in which the projected length is only about 30% of the projected length of one of the extended structures. One helical turn for both helical conformations corresponds to about four double bond segments. On the other hand, conformations with one or more bent-like conformations (cf. Figure 7) also shorten the projected length of the DHA chain as compared to that of the fully extended conformations. These might enable a variation of the projected acyl chain length in analogy with the molecular spring concept.[15]

Conformational Transitions of Acyl Chains: Influence of Polyunsaturation. Let us next return to Figure 6a, which describes the joint probability distribution function for a pair of adjacent dihedral angles of a methylene segment between two double bonds. Note that in the center of the plot, representing a trans,trans conformation for both dihedral angles ($\chi_1 = \chi_2 = 180°$), there is almost zero probability. A single torsion angle can be in a trans conformation (χ_1 or $\chi_2 = 180°$) as long as the adjacent dihedral angle has a skew conformation (χ_1 or $\chi_2 = 120°$, 240°). The conformations with one or two cis torsion angles ($\chi_1 = \chi_2 = 0°$) have zero probability, as can be expected. The origin of these excluded conformations is steric hindrance. Compared to pentane, where exclusion of the (gauche±, gauche∓) conformation in the rotational isomeric model has a major impact, the situation for the pentadiene

fragment considered here is different. The excluded conformations are not among the conformations used to describe the isomeric state of the DHA chain. The result of these excluded conformational regions is that transitions between the major extended conformations, that is, the conformations (±,±), have to occur through the bent conformations (±,∓) as transition states, due to the correlation of the dihedral angles in the analysis of static structures (Figure 6).

Bilayer Membrane Dimensions. Generally, the bilayer structure can be described in terms of the area per lipid and the bilayer repeat distance. The bilayer repeat distance is directly available from small-angle X-ray scattering experiments, but the area per lipid is not directly available.[61] The strength of MD simulations using an *NPT* or *NPγT* ensemble is that a distribution of thermally accessible values of the aqueous interfacial area is sampled. Yet this is also a major weakness, in that the time required to give converged area values, within a range interesting to the experimentalist, is very long. Consequently, to calculate the area per lipid for fully hydrated bilayer membranes, one can combine the ensemble averages from the MD simulations with the results of the ^{2}H NMR experiments, in which the average *sn*-1 chain C−^{2}H order parameters are related to the projected length and area of the chain (cf. Supporting Information). The combined approach allows determination of the bilayer surface area in a considerably shorter simulation time. The basic idea is to apply a correction to the area per lipid from the MD simulations, based on comparison of the averaged order parameters to those from the ^{2}H NMR experiments. An aqueous interfacial area per lipid $\langle A \rangle$ of 71.4 Å^2 is obtained for POPC at 27 °C and 74.8 Å^2 for PDPC at 37 °C, as the NMR-corrected MD simulation area results.

Discussion

Phospholipids containing polyunsaturated fatty acids (PUFAs) have received increased attention in recent years, because they are of vital importance for a large number of biological functions especially involving signal transduction in the nervous system.[65] Such PUFA-containing phospholipids are found as components of cellular membranes and play both a structural and functional role. In the current research, we have employed structural methods capable of providing detailed knowledge of liquid-crystalline biomolecular assemblies, namely ^{2}H NMR spectroscopy and state-of-the-art, molecular dynamics (MD) computer simulations. We report new experimental ^{2}H NMR data, as well as all-atom MD simulations for POPC and PDPC bilayers in the fluid, liquid-crystalline (L_α) state. In this regard, solid-state NMR spectroscopy of liquid-crystalline membranes has the advantage of providing knowledge of second-rank tensorial quantities pertinent to both the average structure and the dynamics of the system. MD simulations, on the other hand, capture the information content of NMR and other experimental observables in terms of the underlying force fields, which can then be utilized to further explore the system of interest.

Here we have combined ^{2}H NMR studies and MD simulations of PUFA-containing lipids in membranes in a complementary fashion. By comparing analogous data for POPC and PDPC, we are now in a position to interpret the solid-state ^{2}H NMR data for PDPC in the L_α phase on an all-atom level. Important issues to be investigated by ^{2}H NMR involve the conformational statistics of the polyunsaturated acyl chains, the orientational ordering of the olefinic C−^{2}H bonds, and their relation to lipid/protein interactions and bilayer properties. Simulated ensemble averages were tested against experimental results for the above bilayers in the L_α state to assess the predictive power of the modeling approach. Profiles of ^{2}H NMR order parameters as well as electron density profiles were calculated from the MD model and compared with the corresponding experimental data. Other structural quantities, not directly available from experiment, were calculated to give new insight into the molecular properties of these biologically important lipids. It is noteworthy that simulations of the POPC bilayer have been carried out by several groups over the past few years.[66−70] However, compared to our model, previous MD simulations of the POPC bilayer utilized a *united-atom* approach, with significantly larger deviations of the predicted order parameter profiles from the experimental values.[66,67,69] A previous simulation using an *all-atom* approach was not described in structural detail.[68] From a recent lattice model simulation of POPC at 27 °C, it was concluded that an area per lipid of 72 Å^2 gave simulated *sn*-1 acyl chain order parameters in agreement with experimental values.[70] This area per lipid and the order parameters for the *sn*-1 acyl chain are in excellent agreement with our findings. However, the order parameter profiles for the *sn*-2 acyl chain obtained from the lattice model[70] deviate significantly from the available experimental values and from our simulated profiles.

How does polyunsaturation influence the physical properties of phospholipid bilayers in the liquid-crystalline state? The major new features of our work can be described as follows. First, the solid-state ^{2}H NMR data show that the configurational properties of the saturated *sn*-1 chain and polyunsaturated *sn*-2 DHA chains of the PDPC bilayer, as compared to those of the POPC bilayer, differ appreciably. We have explained the ^{2}H NMR spectra of the saturated and polyunsaturated acyl chains of the mixed-chain phospholipid bilayers, as well as the electron density profiles, in terms of their configurational properties conferred by the presence of polyunsaturated DHA chains in bilayers. The presence of DHA chains in mixed-chain phospholipids leads to a marked increase in the conformational disorder of the saturated chains. Clearly, the preferred acyl configurations are very different in the two cases, in which specific geometrical aspects must be invoked to explain the results for the PUFA chain. In addition, there is a marked reduction in the number of acyl degrees of freedom for the DHA chain, which can be interpreted in terms of a Ramachandran-type analysis of the dihedral angles.

It is noteworthy that the simulated structural parameters, encompassing the interfacial area, the lamellar repeat distance, and various ^{2}H NMR order parameters for the monounsaturated POPC and the polyunsaturated PDPC bilayers, show reasonable agreement with the available experimental data. The major differences between the POPC and PDPC bilayers can be seen from the *sn*-2 acyl chain order parameter profiles. The S_{CD} order

(65) Bloom, M.; Linseisen, F.; Lloyd-Smith, J. In *Magnetic Resonance and Brain Function: Approaches from Physics*; Maraviglia, B., Ed.; International School of Physics Enrico Fermi: Varenna, Italy, 1998.

(66) Heller, H.; Schaefer, M.; Schulten, K. *J. Phys. Chem.* **1993**, *97*, 8343−8360.
(67) Ceccarelli, M.; Marchi, M. *Biochimie* **1998**, *80*, 415−419.
(68) Armen, R. S.; Uitto, O. D.; Feller, S. E. *Biophys. J.* **1998**, *75*, 734−744.
(69) Chiu, S. W.; Jakobsson, E.; Subramaniam, S.; Scott, H. L. *Biophys. J.* **1999**, *77*, 2462−2469.
(70) Klose, G.; Levine, Y. K. *Langmuir* **2000**, *16*, 671−676.

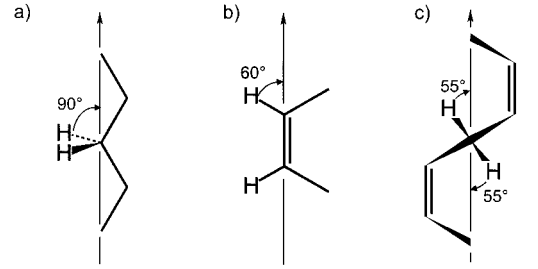

Figure 8. Examples of preferred geometries of C−H bonds in saturated and polyunsaturated acyl chains. (a) Methylene segments of saturated fatty acyl chains; (b) unsaturated vinyl groups of unsaturated and polyunsaturated chains; and (c) polyallylic methylene segments of polyunsaturated chains. The angles between the C−H bond direction and the molecular long axis (arrows) are indicated. Note that the angles of 54.7°, the so-called magic angle, correspond to an orientational order parameter of $S_{CD} = 0$.

parameters of the oleic acyl chains of the POPC bilayer have a similar profile to the saturated *sn*-1 chain, except that next to the double bond the order parameters are small in absolute value. For the PDPC bilayer, all segments of the polyallylic motif have small absolute values of their order parameters. Such order parameters near zero may be a result of substantial orientational disorder or alternatively may be due to the geometric influence of the C−^{2}H bond vector orientations relative to the director axis being near the so-called magic angle of $\beta_{zz} \approx 54.7°$ (see eq 1). This is depicted in Figure 8, in which an interpretation of the small order parameters is given in terms of the covalent bond geometry. For a polymethylene sequence the preferred orientations of the labeled C−^{2}H bond are near 90°, cf. Figure 8a. However, for the vinyl methine deuterons, Figure 8b, and the doubly allylic methylene deuterons, Figure 8c, the C−^{2}H bond vector orientations are near the magic angle, which would yield very small quadrupolar splittings in agreement with the experiment. The conformation for the double allylic methylene group corresponds to those in the extended conformations of the DHA chain. Thus, the bond geometry yields a reduction of the ^{2}H NMR quadrupolar splittings, even if the chains are relatively well ordered along the molecular long axis (indicated by the arrow). In addition, for bilayers of POPC, the C=C bond order parameters of the double bonds from infrared spectroscopy have large positive values, which is consistent with the above geometrical interpretation. Consequently, the double bonds may be rather well aligned relative to the bilayer normal, in agreement with previous considerations.[46]

The global structure of the bilayer can be analyzed in terms of the ensemble-averaged electron density profile, which the MD simulations allow to be resolved in terms of the corresponding group distribution functions along the bilayer normal. Our MD-simulated electron density profiles are in good agreement with the experimental results for the POPC and PDPC bilayers. In both cases, the water distribution functions are similar, but the PDPC bilayer has a slightly increased hydrophobic thickness when compared at the same value of the area per lipid, leading to less water penetration. Consequently, the water electron density profiles overlap less with the hydrocarbon core of the polyunsaturated PDPC bilayer as compared to that of POPC, although the overlap with the unsaturated carbons is greater. A simple interpretation for this observation involves the larger number of unsaturated carbons for PDPC and their positions closer to the lipid headgroup as compared to those of POPC. Note that the observations of a larger hydrophobic thickness and associated exclusion of water from the bilayer center cannot account for a higher apparent permeability for water, as might be suggested by experimental observations for other polyunsaturated lipids.[71]

Next one can ask the following: What are the preferred configurations of the DHA chains in fluid polyunsaturated bilayers? Our work clearly substantiates that helical and angle-iron conformations involving relatively short regions of the DHA chain, for example, triene sequences, are quite abundant.[20,21] Extended helical or angle-iron configurations involving three or more consecutive double bonds of the polyunsaturated DHA acyl chains allow for tight packing of the chains, which might be especially important for the gel phase of these lipids.[16] In the liquid-crystalline (L_α) state, these tend to increase the acyl length while maintaining bilayer fluidity. They represent the major preferred conformations, and we report their probabilities are roughly constant along the chains. The implications of these findings for lipid−protein interactions are such that extended, yet flexible, conformations of the relatively long 22:6 DHA chains may be needed to solvate the hydrophobic surface of the rhodopsin molecule, as suggested by the X-ray crystal structure.[22]

Yet for the entire DHA chains of phospholipids in the fluid L_α state, mixtures of both conformers together with other possible conformers are more likely (cf. Results). Additional conformations with a nonextended shape for the DHA chain are also evident and lead to a looser packing of these lipids, that is, a larger interfacial area. Our MD simulations show that most of the chains have an extended conformation, together with a single bent structure. Moreover, double bent conformations can lead to a hairpin-like shape, or back-folded conformations, of the chain, which yield an increased probability of the terminal methyl group to be found next to the interfacial region of the bilayer. Those nonextended conformations can be observed for a significant fraction of all lipids and increase the average area per lipid as compared to that of POPC. A simple geometric measure of this back bending is the distance of the terminal methyl group relative to atoms in the interfacial region, such as the carbonyl carbons, which can also be observed in the MD trajectories. Interestingly, the hairpin-like conformations have a relatively long lifetime, on the order of a few hundred picoseconds. This leads to a pronounced memory effect for the membrane bilayer and might be a structural correlate of the observed thermal hysteresis.[16] Large conformational changes would be necessary to change these frozen-in hairpin-like conformations back to extended conformations. However, this would necessitate a diffusion mechanism, whose kinetics are limited by the concentration of spontaneous void volumes in bilayer membranes. Such a dynamical memory effect could lead to significant microstructural and dynamical heterogenity of polyunsaturated lipids at ambient temperature, as observed for the simulated bilayers. The less unsaturated POPC bilayer membranes are lacking such structural heterogenity and show only a small variation in the average values for the area per lipid at constant surface tension for different simulations. In this sense, the monounsaturated POPC bilayer is more like a saturated lipid bilayer, such as DPPC.

Another aspect of interest is that the potential energy barriers for rotational isomerization of the polyunsaturated acyl groups

(71) Olbrich, K.; Rawicz, W.; Needham, D.; Evans, E. *Biophys. J.* **2000**, *79*, 321−327.

are relatively small in comparison to saturated polyethylene chains. This might be correlated with the bending rigidity κ and/or the area elastic modulus K_a of the membrane bilayer.[72,73] These properties of the hydrocarbon region of PUFA-containing lipid bilayers are important with regard to film properties and have been discussed in the context of lipid modulation of the meta I−meta II conformation equilibrium of rhodopsin.[13,72] The relation of the averaged order parameter $\langle|S_{CD}|\rangle$ to the area per lipid is experimentally very important.[44] For instance, area changes in relation to different osmotic pressures are used to estimate the lateral compressibility moduli of membranes.[74] In recent work on differences of the unsaturated SOPC and polyunsaturated SDPC lipid bilayers, a significant difference between the NMR and X-ray derived area compressibility moduli K_a has been detected, with the NMR value being higher than the X-ray value for the polyunsaturated SDPC bilayer, but equal for SOPC. (Note the area elastic modulus K_a is the reciprocal of the lateral compressibility; a softer bilayer has a smaller area elastic modulus and vice versa.) The problem arising from these data is that NMR suggests an increase in the area compressibility modulus for the polyunsaturated SDPC bilayer, as compared to those of saturated and monounsaturated phosphatidylcholine (PC) lipids, whereas X-ray studies yield a lower area compressibility modulus.[74] In the present work, we calculated K_a for the polyunsaturated PDPC bilayer from the MD-simulated ensembles at different applied surface tensions. The area compressibility modulus of $K_a = 0.38$ J m^{-2} determined in this manner for PDPC, at 25.4 waters per lipid and 37 °C, indicated a decreased compressibility as compared to that of the saturated DPPC lipid bilayer in the liquid-crystalline state at 50 °C, with values of $K_a = 0.26$ and 0.30 J m^{-2} calculated from MD simulations.[48,54] For the SDPC bilayer, the experimental results are 0.12 J m^{-2} from X-ray data, which is methodologically similar to our direct MD method (vide supra), as compared to the indirect ^{2}H NMR method, which uses the experimental averaged order parameter $\langle|S_{CD}|\rangle$ to calculate the area per lipid.[44] From the experimental NMR data for SDPC, a value of 0.31 J m^{-2} was derived. The area compressibility modulus of PDPC from our MD simulations is thus slightly higher, but still in agreement, with experimental values for the homologous lipid SDPC at 30 °C. Our conclusion of a smaller compressibility for the bilayers containing polyunsaturated DHA acyl chains can be viewed as a somewhat greater rigidity of such membranes. The biological significance of this observation might be associated with the high abundance of polyunsaturated lipids in membranes, where changes in the bilayer interfacial area and thickness are perhaps necessary to adapt to the hydrophobic surface of membrane proteins during conformational changes, as in the case of the meta I−meta II transition of rhodopsin.[72,75]

In summary, this work has entailed the application of ^{2}H NMR, in combination with all-atom molecular dynamics simulation methods, to bilayers of highly polyunsaturated lipids containing docosahexaenoic acid (DHA). The results of some of the first MD simulations of highly polyunsaturated bilayers are reported. Additional MD simulations of the effects of polyunsaturation have recently appeared.[76] Our studies of the influences of acyl chain unsaturation have revealed the conformational properties of both the saturated and the polyunsaturated chains of mixed-chain phospholipids differ significantly from those of less unsaturated systems. Overall, these features are suggestive of the particular relevance of polyunsaturated lipids for the proper functioning of membrane proteins. This research provides a structural basis for studies of the interactions of polyunsaturated lipids with G protein-coupled receptors, such as rhodopsin. Clearly, further structural studies of these biologically important molecules are vital to understanding their roles in key biomembrane functions.

Acknowledgment. This work was supported by the U. S. National Institutes of Health (EY 12049) and by the Deutsche Forschungsgemeinschaft (Sonderforschungsbereich 266-B12). We also would like to thank Dr. Horia Petrache for many helpful discussions during the course of this work.

Supporting Information Available: Use of combined molecular dynamics (MD) and ^{2}H NMR data to calculate average bilayer dimensions; structural results for unsaturated and polyunsaturated lipid bilayers in the L_α state (PDF). This material is available free of charge via the Internet at http://pubs.acs.org.

JA011383J

(72) Gibson, N. J.; Brown, M. F. *Biochemistry* **1993**, *32*, 2438−2454.
(73) Brown, M. F. *Chem. Phys. Lipids* **1994**, *73*, 159−180.
(74) Koenig, B. W.; Strey, H. H.; Gawrisch, K. *Biophys. J.* **1997**, *73*, 1954−1966.
(75) Wiedmann, T. S.; Pates, R. D.; Beach, J. M.; Salmon, A.; Brown, M. F. *Biochemistry* **1988**, *27*, 6469−6474.
(76) Saiz, L.; Klein, M. L. *J. Am. Chem. Soc.* **2001**, *123*, 7381−7387.
(77) Perly, B.; Smith, I. C. P.; Jarrell, H. C. *Biochemistry* **1985**, *24*, 1055−1063.
(78) Hong, M.; Schmidt-Rohr, K.; Nanz, D. *Biophys. J.* **1995**, *69*, 1939−1950.